Received: 7 October 2022 | Accepted: 2 November 2022

DOI: 10.1002/pamm.202200114

Dynamic Crack Propagation in a Lattice Boltzmann Method for Solid Mechanics

Henning Müller[1,*], **Alexander Schlüter**[2], and **Ralf Müller**[1]

[1] Institute for Mechanics, TU Darmstadt, Franziska-Braun-Straße 7, D-64287 Darmstadt

[2] Institute of Applied Mechanics, TU Kaiserslautern, P.O. Box 3049, D-67653 Kaiserslautern

In recent years, Lattice Boltzmann methods (LBMs) have been adapted and developed to simulate the behavior of solids. They have already been applied to fractures as well. However, until now, our previous work has been restricted to stationary cracks.

In this work, we regard the reduced 2D case of anti-plane shear deformation with mode III crack opening. The wave equation is the governing equation for this problem, which is solved via an LBM.

The main contribution of this work is the introduction of an algorithm to handle crack growth in an LBM for solids. The underlying scheme is based on geometric assumptions, which is well suited for the regular lattice used by the LBM. A fracture criterion based on the stress intensity factor is implemented and illustrated by a numerical example.

1 Introduction

Lattice Boltzmann methods (LBMs) can be used as numerical solvers for various partial differential equations [1, 2], well beyond the field of fluid dynamics, for which they were initially conceived. They have the advantage of a meshless method, only requiring a regular lattice, with explicit and locally defined operations. This promises great performance, especially when combined with parallel computing [3].

Recently, an effort has been made towards the development of LBMs for solid mechanics. An overview of recent developments and relevant literature regarding this topic can be found e.g. in [4].

One approach is to rewrite the dynamics of the solid body in terms of wave equations. In 2D, a decomposition into longitudinal and transverse waves can be used for plane strain [5]. Similarly, the problem can be reduced to anti-plane shear deformation [6]. The anti-plane shear model has already successfully been applied to a stationary crack. The main feature is the consideration of non–lattice conforming boundary conditions [4]. This can now be extended further to model the growth of cracks.

In this work, the underlying scheme and the algorithmic approach are presented. The crack is represented in a geometric manner. It is independent of the lattice itself, beyond the pure geometry of the discretization. In a post-processing step, information about the configuration at the lattice sites is used to determine the parameters, which are relevant to the evaluation of the fracture criterion. The algorithm concentrates on a few lattice points in the direct vicinity of the crack and thus retains the good efficiency of LB methods.

This work first introduces some background information on the LBM for anti-plane shear in Sec. 2. Then the processing scheme and the algorithm for dynamic crack propagation are shown in Sec. 3, with additional information on the evaluation of stress intensity factors and the fracture criterion. Next, a numerical example in Sec. 4 illustrates the prospects of this method and acts as a proof-of-concept for the algorithm. Lastly, a discussion of the results and concluding remarks on the possibilities of generalization follow.

2 Lattice Boltzmann Method for Anti-plane Shear Deformation

A linear elastic solid is considered. Furthermore, small deformations and a restriction to the 2D case are assumed. This can be described by the Navier-Cauchy equation. Only the x-y-plane is regarded and both the displacement and loading are restricted to the out-of-plane direction along the z-axis. For such a system, the Navier-Cauchy equation reduces to a 2D wave equation for the displacement component $w(x, y, t)$. This problem can then be solved by an LBM, e.g. the scheme proposed by Yan [7]. The domain is discretized by a regular lattice with spacing Δh and timestep Δt.

In this section, only a short overview of the employed LBM is given. For a more in-depth description of this method and its application to solid mechanics, see [6], while a general introduction to LBMs can be found in textbooks such as [1, 8].

Generally, an LBM works on the basis of distribution functions f^α, which are manipulated locally. The index α relates to an element of a discrete velocity set $\boldsymbol{c}^\alpha$ with $|\boldsymbol{c}^\alpha| = {}^{\Delta h}/_{\Delta t}$.

* Corresponding author: e-mail henning.mueller@tu-darmstadt.de, phone +49 6151 16 22748

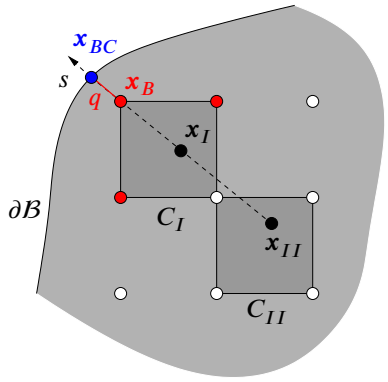

Fig. 1 Depiction of the macroscopic strategy for non–lattice conforming boundary conditions at the boundary point x_B. The interpolation involves the prescribed boundary value at the closest point $\boldsymbol{x}_{BC}$ on the boundary, as well as the displacement at x_I and x_{II}, which in turn result from bilinear interpolation in the cells C_I and C_{II}; from [4].

The discrete Lattice Boltzmann equation (LBE) with a BGKW-collision operator [9, 10] is given by

$$f^\alpha\left(\boldsymbol{x}+\boldsymbol{c}^\alpha\Delta t, t+\Delta t\right) = f^\alpha(\boldsymbol{x},t) - \frac{1}{\tau}\left[f^\alpha(\boldsymbol{x},t) - f^\alpha_{\text{eq}}(\boldsymbol{x},t)\right], \tag{1}$$

where f_{eq} describes equilibrium distributions and τ the relaxation time. A simple D2Q5–velocity scheme is used here, thus $\alpha \in \{0,1,2,3,4\}$.

For Yan's method, the central moment is connected to the rate of change in the displacement

$$\left[\sum_\alpha f^\alpha\right] = \frac{\partial w}{\partial t} = \dot{w}, \tag{2}$$

and the equilibrium distributions are defined as

$$f^0_{\text{eq}} = \frac{\partial w}{\partial t} - \frac{2\lambda w}{c^2} \quad \text{and} \quad f^\alpha_{\text{eq}} = \frac{\lambda w}{c^2} \quad \text{for } \alpha \in \{1,2,3,4\}, \quad \text{with} \quad \lambda = \frac{c_s^2}{\Delta t}\left[\tau - \frac{1}{2}\right]_{-1} \tag{3}$$

where $c = {}^{\Delta h}/_{\Delta t}$ is related to the shear wave speed. Finally, to obtain the displacement, a simple forward Euler time integration is used

$$w(\boldsymbol{x}, t+\Delta t) = w(\boldsymbol{x},t) + \Delta t\, \dot{w}(\boldsymbol{x}, t+\Delta t). \tag{4}$$

2.1 Non-Lattice Conforming Boundary Conditions

At a boundary, some neighbors of a lattice point might not exist and no distributions are streamed from beyond this boundary. These missing distribution functions need to be determined from the prescribed boundary conditions. Thus, the boundary conditions at the macroscale need to be converted to the distribution functions at the mesoscale. Here, the macroscopic strategy described in [4] is employed. Only some basic information is provided here as background to the last step of the scheme in Sec. 3.

In short, a quadratic interpolation is used to find the displacement w_B at a boundary lattice point $\boldsymbol{x}_B$, cf. Fig. 1. Due to the coupled contributions of other boundary lattice points, this leads to a linear system of equations

$$\boldsymbol{S}\boldsymbol{w}_B(t+\Delta t) = \boldsymbol{R}(t+\Delta t), \tag{5}$$

which can be solved to get the displacement of all boundary lattice points. With the results for w_B, each of the m missing distributions at $\boldsymbol{x}_B$ can be set via the formula

$$f^\alpha(\boldsymbol{x}_B, t+\Delta t) = \frac{1}{m}\left[\frac{w(\boldsymbol{x}_B, t+\Delta t) - w(\boldsymbol{x}_B,t)}{\Delta t} - \left[\sum_{\beta\in\mathcal{N}_B} f^\beta(\boldsymbol{x}_B, t+\Delta t)\right]\right], \quad \forall \alpha \notin \mathcal{N}_B, \tag{6}$$

where $\mathcal{N}_B$ describes the set of indices which denote links to interior neighbouring lattice points of $\boldsymbol{x}_B$.

3 Algorithm for Crack Propagation

The handling of crack growth occurs as an additional step in the LB algorithm, which is appended at the end of a time step of the time loop, after all field values at the lattice sites have been updated. A fracture criterion can then be evaluated based on these field values. Details on the chosen criterion and its implementation can be found in Sec. 3.1, whereas a more general description is given here.

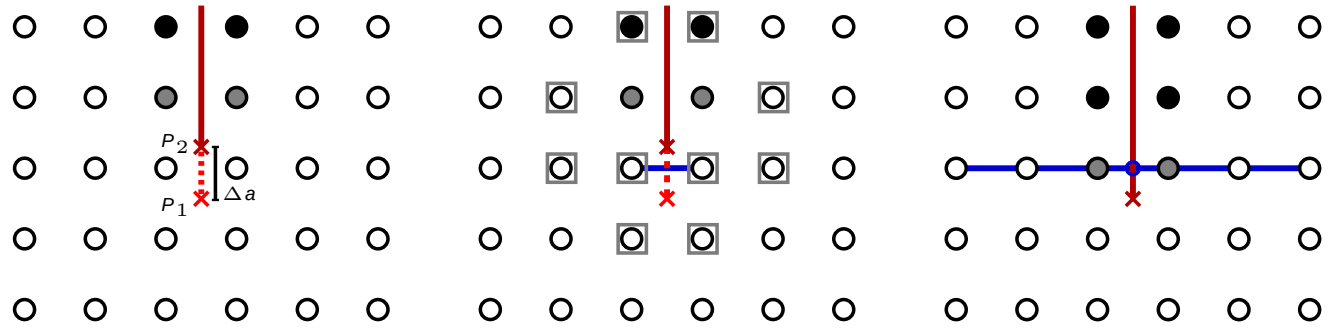

(a) Crack gowth: The crack is extended by a segment (dotted line) of length $\Delta a = \dot{a}\,\Delta t$, with P_1 as the new crack tip.

(b) Boundary point identification: For finding the intersected link (blue line), all links connected to points in gray boxes are successively checked.

(c) Boundary processing: The new boundary points are processed. The interpolation involves the points on the blue line, including the closest point on the crack.

Fig. 2: Handling of a growing crack (dark red) in three steps, including the processing of boundary points (filled circles).

An initial crack needs to be present in the domain. This crack itself is represented as a line between two points, see the red line in Fig. 2. The algorithmic treatment of crack propagation follows Alg. 1, which can be split up into three steps. These are illustrated in Fig. 2. First the criterion is evaluated. If it is fulfilled, the crack tip is shifted by $\Delta \boldsymbol{a} = \dot{a}\Delta t \boldsymbol{d}$, where $\dot{a}$ is the current rate of crack growth and $\boldsymbol{d}$ is the direction. This creates a new crack segment, see Fig. 2a. It would be possible to compute both $\dot{a}$ and $\boldsymbol{d}$ during runtime based on the current configuration. For simplicity, only straight cracks are regarded for now, i.e. $\boldsymbol{d}$ is constant and given as input.

Algorithm 1 Handling of dynamic cracks in the LBM

procedure CRACKGROWTH
  propagation ← EVALUATECRITERION
  if propagation = `True` **then**
    $\vec{v} \leftarrow \dot{a} \cdot \vec{\hat{d}}$
    cr_tip$_{\text{prev}}$ ← cr_tip
    cr_tip ← cr_tip $+ \vec{v}\,\Delta t$
    create cr_segment(cr_tip$_{\text{prev}}$ □ cr_tip) ▷ new crack segment
    $B \leftarrow$ CHECKLINKS(cr_segment)
    PROCESSPOINTS(B)
  end if
end procedure
function CHECKLINKS(cr_segment)
  let $\mathcal{N}(p)$ be the set of neighbors linked to lattice points p
  let (B_{prev}) be the set of boundary points from previous increment
  $Q \leftarrow \mathcal{N}(B_{\text{prev}})$ ▷ queue
  $B \leftarrow \emptyset$ ▷ new boundary points
  $V \leftarrow \emptyset$ ▷ visited
  while $|Q| > 0$ **do**
    let $p \in Q$
    $Q \leftarrow Q \backslash \{p\}$ ▷ pop p from queue
    $V \leftarrow V \cup \{p\}$ ▷ mark as visited
    for all $n_p \in \mathcal{N}(p)$ **do**
      create link(p □ $n_p 2$)
      if cr_segment intersects link(p □ n_p) **then**
        $B \leftarrow B \cup \{p, n_p\}$
        $Q \leftarrow Q \cup \mathcal{N}(n_p) \backslash V$
      end if
    end for
  end while
  return B
end function

The crack segment should act as traction free boundary within the domain. Thus the connectivity of lattice points in the vicinity of the crack segment might require modification. In order to identify any of these lattice points, which are adjacent to the segment, the links connecting a point to its neighbors need to be checked. This identification process can be narrowed to down to an environment around the previous crack tip, indicated by grey boxes in Fig. 2b. The function `CheckLinks` in Alg. 1 shows the approach of an environment that is dynamically updated. If the crack segment intersects any link, this link is broken, inhibiting the exchange of distribution functions in subsequent streaming steps. Instead, the distributions for these links are determined from the boundary conditions. To this end, the previously linked lattice points must be processed accordingly. For the macroscopic strategy presented in [4], see also Sec. 2.1, the interpolation scheme needs to be instituted with the required coefficients. This adds new equations to the system described by Eq. (5). Thus the matrix $\boldsymbol{S}$ and the vector $\boldsymbol{R}$ in Eq. (5) need to be appended accordingly and $\boldsymbol{S}$ must be inverted to solve the system of equations. In the next time step these points are then treated as boundary lattice points.

3.1 Stress Intensity Factors and the Fracture Criterion

In this section the implementation of one fracture criterion is discussed. It is based on stress intensity factors (SIF) and was first formulated by Irwin [11]. In the immediate vicinity of the crack tip, the elastic fields exhibit a universal shape with certain unique parameters determining its amplitudes. These parameters are the SIFs K_I, K_{II} and K_{III} for the three different crack opening modes. Since the mechanical model is limited to anti-plane shear deformation, only K_{III} is regarded and the index omitted in the following.

With Irwin's criterion, the crack propagates when K reaches a certain critical value K_C, a material specific parameter, which is passed as input to the algorithm. This can be formulated as

$$K > K_C. \tag{7}$$

K is evaluated from the jump in the displacement $\delta = |w_L(r_0) - w_R(r_0)|$ between both crack faces (L and R) for a very small distance r_0 from the crack tip, where $r_0 \ll L$ for a characteristic length L of the system, such as as the total crack length. For stationary problems, it can be computed via

$$K(r_0) = \frac{\mu}{4}\sqrt{\frac{2\pi}{r_0}}\,\delta, \tag{8}$$

with the shear modulus μ.

For dynamical problems, however, K has to be adjusted [12] by a factor to compensate dynamical effects of a moving crack tip. Instead, due to practical reasons, an approach is taken, which adapts the distance of evaluation is to the crack speed v. K is sensitive to variations in r, thus partially compensating for the effects of crack propagation. It is assumed, that

$$K^{\text{dyn}}(t) \simeq K^{\text{inst}}(r)\big|_{t}, \quad r(v) \approx r_0, \tag{9}$$

with the instantaneous value of K at time t from Eq. (8) and the relative crack speed $v = \dot{a}/c_s$. The distance of evaluation is and the relative speed v are estimated from

$$r(v) \approx \frac{r_0}{1-v}, \quad \text{and} \quad v\,(K; K_C) \sim \tanh\sqrt{(K/K_C)^4 - 1}\; v_{\max}, \quad K > K_C,\ 0 < v \le v_{\max}, \tag{10}$$

where v is based on the relative overshoot of K over K_C, with the maximum allowed speed $v_{\max}$. It should be noted, that the expressions in Eq. (10) are chosen from empirical considerations to minimize the the overshoot of K over K_C.

4 Numerical Example

A simple numerical example is given here as an illustration of crack growth and as a proof of concept for the algorithm, including the criterion and the implementation presented in the preceding section. The domain shown in Fig. 3 is rectangular, except for a V-shaped notch. It is held fixed at the right edge (purple), while the top, bottom, and left edge are treated as free boundaries. A short initial crack, originating from the notch, is allowed to propagate horizontally.

A traction is applied to the flanks of the notch. This is modulated in time by a sine (blue) or a cosine (green), respectively, see Fig. 4. This loading excites waves in the domain, effectively causing the crack to be periodically pulled apart.

The spatial discretization is chosen as $\Delta h = L/32$ for an arbitrary length L. This results in a total of $4\,000$ lattice points. The simulation runs for a time $0 < t < 20\,L/c_s$ and the maximum relative speed for the crack propagation is set to $v_{\max} = 0.9$.

The results of this example are summarized in Fig. 5. The figure shows K as a reaction to the waves travelling through the material. This is indicated by K rising and falling again, giving three wide peaks. For each on,e K eventually surpasses the critical value. This results in periods of crack propagation, during which K stays close to or slightly above K_C. However, the propagation is not continuous. It also temporarily halts throughout these periods and comes to a stop after K falls below K_C.

Illustrations of the deformed domain for different times are given in Fig. 6. The crack grows significantly in length, which can especially be seen when comparing Fig. 6b to 6d. Furthermore, Fig. 5 shows that the length a of the crack increases, just as the speed v is at a positive value, directly corresponding to the periods of growth with $K > K_C$.

In conclusion, the features outlined above reflect the behavior expected during crack propagation.

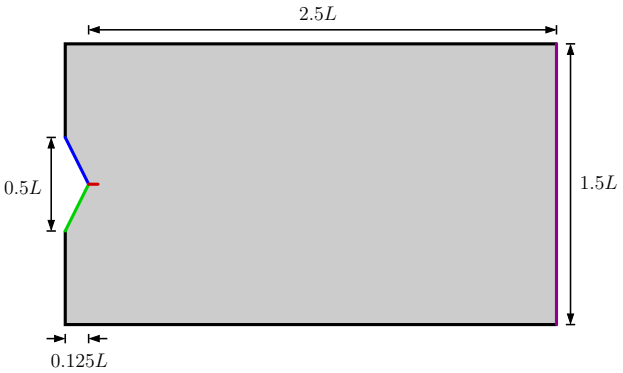

Fig. 3: The domain for the numerical example with L as an arbitrary length scale. The initial crack (red) has a length of $0.16L$. At the flanks of the notch, a time dependent traction is applied.

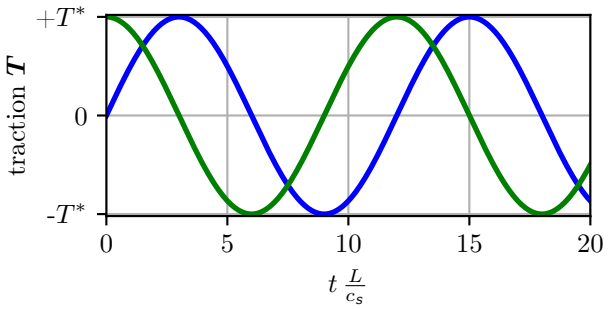

Fig. 4: The time dependency of the applied traction at the notch. The colors correspond to the edges in Fig. 3.

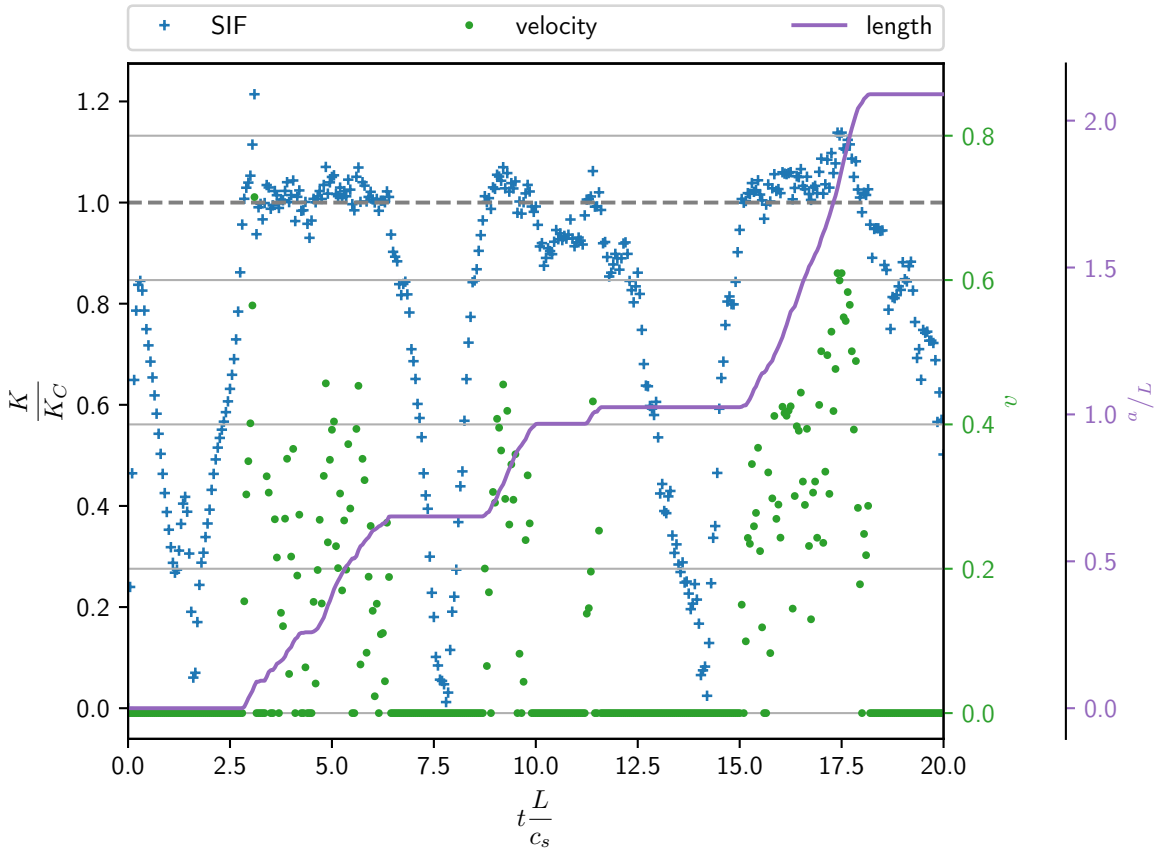

Fig. 5: Results of the numerical example. The blue crosses show the stress intensity factor K. When it surpasses the critical value, normalized to 1 here, the crack grows. The relative crack speed $v = \dot{a}/c_s$ (green dots) is then positive and the additional length of the crack (purple line) increases.

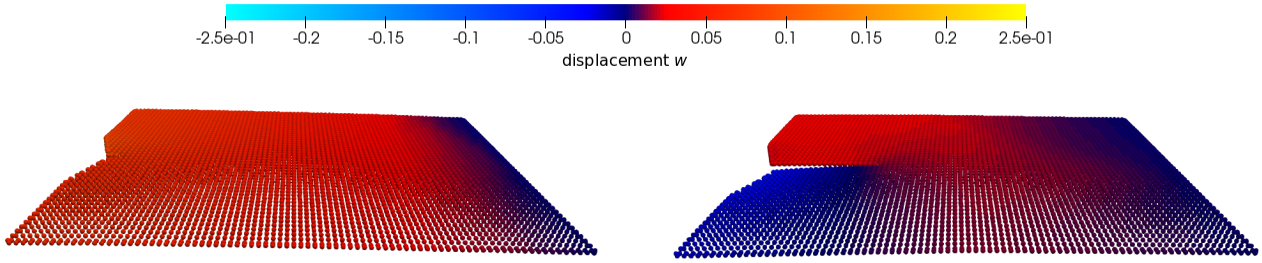

(a) $t = 3.0$ **(b)** $t = 6.5$

(c) $t = 15.0$ **(d)** $t = 18.0$

Fig. 6: Illustrations of the deformed domain. The color map represents the scalar value of displacement field w. In (a), the crack just begins to grow before it is pulled apart further. (b) shows the crack at the the end of the first peak in Fig. 5, after propagation has halted. (c) is at the beginning of the third period of crack growth, while (d) shows its end, with a considerably longer crack.

5 Conclusion and Discussion

This work presents a novel method to simulate crack propagation, added onto a LBM for anti-plane shear deformation. The scheme is based on geometrical considerations, which take advantage of the simple regular lattice. Crack propagation is appended as a post-processing step to the existing LBM. It does not add much complexity, such as additional equations or a remeshing.

The numerical example shows the expected behavior and indicates that the underlying concept is indeed working as intended. Still, more extensive studies and comparisons to established methods are needed in order to verify the performance and efficiency of the method.

The evaluation of the SIF K remains challenging. However this evaluation, as well as the criterion, can be reformulated or exchanged without any changes to the schematic approach. These modular characteristics of the algorithm also allow for possible a generalizations beyond anti-plane shear deformation and mode III crack opening. At the lattice points, only the data relevant to the evaluation of the criterion is needed. Therefore, the specific LB scheme can be exchanged, since the definition of statistical moments or the computations themselves are not relevant to the algorithm handling the crack propagation. For a different mechanical model, such as plane strain with crack opening modes I and II, the necessary evaluations, the crack propagation criterion, as well as the boundary handling need to be adjusted, which should pose no problem with the method proposed here.

In summary, this approach to crack propagation is more universal than the restricted model shown here.

Acknowledgements Open access funding enabled and organized by Projekt DEAL. The authors gratefully acknowledge the funding by the German Research Foundation (DFG) within the project 423809639.

References

[1] S. Succi, The Lattice Boltzmann equation: for complex states of flowing matter (Oxford University Press, Oxford, 2018).
[2] S. Simonis, M. Frank, and M. J. Krause, Philos. Trans. R. Soc., A **378**(2175), 20190400 (2020).
[3] L. Pastewka and A. Greiner, HPC with Python (Universitätsbibliothek Tübingen, 2019).
[4] A. Schlüter, H. Müller, and R. Müller, Arch Appl Mech(August) (2022).
[5] A. Schlüter, H. Müller, and R. Müller, PAMM **21**(December) (2021).
[6] A. Schlüter, C. Kuhn, and R. Müller, Comput Mech **62**(5), 1059–1069 (2018).
[7] G. Yan, Journal of Computational Physics **161**(1), 61–69 (2000).
[8] T. Krüger et al., The Lattice Boltzmann Method: Principles and Practice (Springer International Publishing, Cham, 2017).
[9] P. L. Bhatnagar, E. P. Gross, and M. Krook, Phys. Rev. **94**(3), 511–525 (1954).
[10] P. Welander, Arkiv fysik **7** (1954).
[11] G. R. Irwin, Journal of Applied Mechanics **24**(3), 361–364 (1957).
[12] L. B. Freund, Dynamic fracture mechanics (Cambridge University Press, Cambridge ; New York, 1990).

